PMD-Induced Crosstalk in Ultrahigh-Speed Polarization-Multiplexed Optical Transmission in the Presence of PDL

Toshihiko Hirooka, *Member, IEEE*, Toshiyuki Hirano, Yutaro Tomiyama, Pengyu Guan, *Student Member, IEEE*, and Masataka Nakazawa, *Fellow, IEEE*

***Abstract*—We present a new type of crosstalk in a polarization-multiplexed ultrahigh-speed transmission caused by polarization-mode dispersion (PMD) in the presence of polarization-dependent loss (PDL). When PMD and PDL are both present, the orthogonality between two principal states of polarization (PSP) is reduced. As a result, crosstalk inevitably occurs between two polarizations and prevents the two channels from being separated completely during polarization demultiplexing. The system impact of these effects in a polarization-multiplexed terabit/s transmission is also demonstrated experimentally.**

***Index Terms*—High-speed optical pulse transmission, optical time-division multiplexing, polarization-dependent loss, polarization-mode dispersion, polarization multiplexing, ultrashort optical pulse.**

I. Introduction

With the huge growth in Internet traffic, it has become increasingly important to realize an ultrahigh-speed backbone network that can accommodate large volumes of data without congestion. In particular, increasing the bit rate per wavelength channel will enable us to realize future ultrahigh-capacity optical networks with a simple configuration, great flexibility, and low power consumption due to the need for fewer wavelength channels. By adopting optical time division multiplexing (OTDM) [1], a symbol rate as fast as 640 Gbaud per polarization has been demonstrated in a single carrier, where the bit rate is increased to 1.28 Tbit/s by using polarization multiplexing [2] and to 2.56 Tbit/s by additionally employing a DQPSK modulation [3].

Polarization multiplexing is an easy and useful way of doubling the bit rate under a fixed symbol rate, or equivalently, doubling the spectral efficiency. In an ideal optical fiber, two orthogonal polarization channels can be transmitted independently without coupling with each other. However, real optical fibers exhibit random birefringence due to geometrical perturbations or nonsymmetrical stress, and this leads to polarization-mode dispersion (PMD) [4], [5]. PMD causes frequency-dependent state of polarization (SOP) variation inside the signal bandwidth, and this results in a differential group delay (DGD) between the two principal states of polarization (PSP). DGD can be avoided by matching the SOP of the launched signal to the PSP itself. However, even when first-order PMD is completely compensated, second-order PMD becomes problematic for a large signal bandwidth such as in a long-haul transmission of ultrashort optical pulses. Second-order PMD is represented as the frequency dependence of DGD and PSP, which results in polarization-dependent chromatic dispersion and depolarization, respectively [6], [7]. In addition, optical components such as optical amplifiers, isolators, and couplers exhibit polarization-dependent loss (PDL), which leads to optical power variations depending on the SOP.

In this paper, we show that, in the presence of both PMD and PDL, detrimental impairments occur in ultrahigh-speed polarization-multiplexed transmission. A major consequence of their interplay is a reduction of the orthogonality between two PSPs [8]. This phenomenon imposes severe limitations on polarization-multiplexed transmission because it prevents the two channels from being completely separated at the receiver due to mode coupling. The combined effect of PMD and PDL has been intensively studied both analytically and experimentally, such as waveform distortions [9] and OSNR degradation [10]. System impact of PDL impairments in coherent transmission has also been a recent subject of concern [11], [12]. PMD and PDL may be treated separately for PDL values of practical interest, as far as the transmission bandwidth is not significantly large. Here, we consider a case with ultrashort pulse transmission, in which the frequency dependence of PMD within a signal bandwidth is not neglected. We shall describe analytically the crosstalk that occurs at the polarization demultiplexing, and show that the degradation is particularly disadvantageous for ultrashort pulse propagation. We also demonstrate a polarization-multiplexed transmission of ultrashort optical pulses and identify the impairment experimentally. Coherent detection for such an ultrashort pulse has been demonstrated [13]–[15], but the influence of PDL in ultrahigh-speed coherent transmission and its mitigation with DSP remain for future work.

This paper is organized as follows. In Section II, we provide an analytical description of PMD and PDL. The PSP nonorthogonality and crosstalk induced by the interplay between PMD and PDL during polarization-multiplexed ultrashort pulse propagation are presented in Section III. Finally, in Section IV, the system impact of these effects on polarization-multiplexed Terabit/s/channel transmission is described in detail.

Manuscript received March 05, 2011; revised June 20, 2011; accepted July 28, 2011. Date of publication August 04, 2011; date of current version September 14, 2011.

The authors are with the Research Institute of Electrical Communication, Tohoku University, Sendai 980-8577, Japan (e-mail: hirooka@riec.tohoku.ac.jp).

Digital Object Identifier 10.1109/JLT.2011.2163617

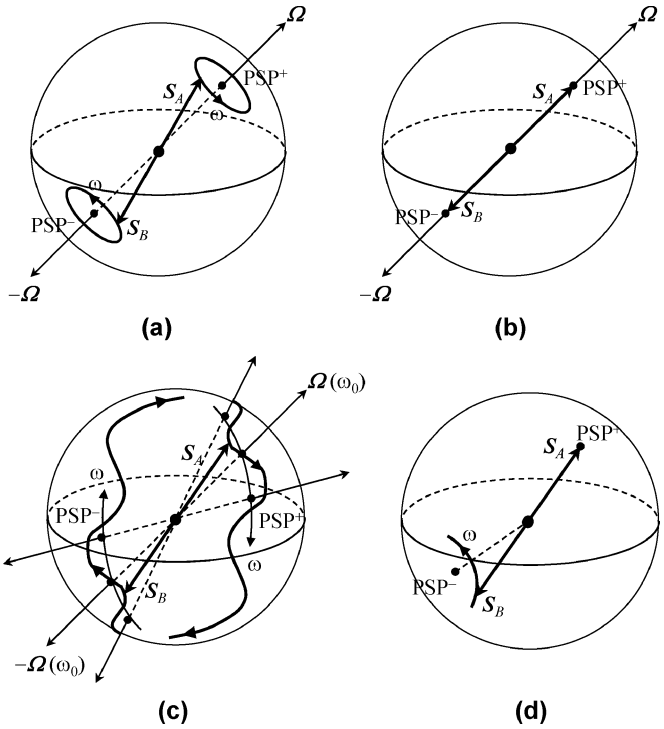

Fig. 1. The relationship between Stokes vectors for two orthogonal polarizations, $\boldsymbol{S}_A$ and $\boldsymbol{S}_B$, PMD vector $\boldsymbol{\Omega}$, and PSP on a Poincaré sphere in the presence of various forms of PMD and PDL. (a) First-order PMD, (b) first-order PMD when $\boldsymbol{S}_A$ and $\boldsymbol{S}_B$ are matched to PSP, (c) second-order PMD, and (d) PDL.

II. Theory

A. Analytical Description of PMD and PDL

To clarify the impairments caused by PMD and PDL, here we review their analytical description based on a Stokes vector on a Poincaré sphere. We first consider the case without PDL. PMD is described as a frequency-dependent SOP at the output of a fiber, which is represented by the following equation in the frequency domain [4], [5]:

$$\frac{d\boldsymbol{S}}{d\omega} = \boldsymbol{\Omega} \times \boldsymbol{S} \tag{1}$$

where $\boldsymbol{S}$ is a Stokes vector representing the output SOP, and $\boldsymbol{\Omega}$, known as a PMD vector, has a magnitude equivalent to a DGD, $\Delta\tau$, and a direction along the rotation axis of $\boldsymbol{S}$, which we define as $\boldsymbol{q}$:

$$\boldsymbol{\Omega} = (\Delta\tau)\,\boldsymbol{q}. \tag{2}$$

Fig. 1(a) shows the relationship between $\boldsymbol{S}$ and $\boldsymbol{\Omega}$ on a Poincaré sphere. Here, $\boldsymbol{S}_A$ and $\boldsymbol{S}_B$ are Stokes vectors corresponding to the SOP of two channels in a polarization-multiplexed transmission. Because of their orthogonality, they have opposite directions on a Poincaré sphere. The SOP defined as the intersecting point of $\boldsymbol{\Omega}$ on a Poincaré sphere is referred to as PSP. As long as $\boldsymbol{\Omega}$ is a constant vector with respect to ω, the Stokes vector traces a circular arc around $\boldsymbol{\Omega}$ as shown in Fig. 1(a). In particular, when the SOP matches PSP, namely $\boldsymbol{\Omega} \times \boldsymbol{S} = 0$, the Stokes vector remains constant regardless of ω, as can be easily seen from (1) and plotted in Fig. 1(b). This indicates that no DGD is caused by launching the signal along the PSP and therefore the first-order PMD can be compensated for completely in principle.

On the other hand, for an ultrashort optical pulse, the frequency dependence of $\boldsymbol{\Omega}$ cannot be neglected because of the broad signal bandwidth $\Delta\omega$. As a result, the Stokes vector trace becomes very complicated, as shown schematically in Fig. 1(c). This can be clearly seen from a Taylor series expansion of $\boldsymbol{\Omega}(\omega_0)$ around a center frequency ω_0:

$$\boldsymbol{\Omega}(\omega) = \boldsymbol{\Omega}(\omega_0) + \left(\frac{d(\Delta\tau)}{d\omega}\boldsymbol{q} + \Delta\tau\frac{d\boldsymbol{q}}{d\omega}\right)\Delta\omega \tag{3}$$

where $\Delta\omega = \omega - \omega_0$ corresponds to the signal bandwidth. The terms proportional to $\Delta\omega$ on the right-hand side of (3) represent the second-order PMD. Of the two contributions, the first term describes the frequency dependence of the DGD, which is referred to as polarization-dependent chromatic dispersion (PCD). This indicates that the fiber has a different GVD along the two PSPs. The latter term is referred to as depolarization, and indicates that the PSP varies with frequency. It may even be possible that the PSP vector is rotated by 180 deg. from a center frequency within a signal bandwidth on a Poincaré sphere, and hence the SOP at a certain frequency component may become orthogonal to the SOP at another frequency inside the spectrum. This leads to crosstalk in a polarization-multiplexed transmission. However, in the following we shall discuss more a detrimental effect that occurs when the second-order PMD is combined with PDL.

When PDL also exists in the transmission link, the PMD vector should be treated as a complex vector, $\boldsymbol{\Omega}+i\boldsymbol{\Lambda}$. The evolution of a Stokes vector in the frequency domain in the presence of both PMD and PDL is derived in [16] and given by

$$\frac{d\boldsymbol{S}}{d\omega} = \boldsymbol{\Omega} \times \boldsymbol{S} - (\boldsymbol{\Lambda} \times \boldsymbol{S}) \times \boldsymbol{S}. \tag{4}$$

This indicates that, even when $\boldsymbol{S}$ is set parallel to $\boldsymbol{\Omega}$, the Stokes vector is no longer frequency-independent. Instead, the PSP in the present case can be found from the condition $d\boldsymbol{S}/d\omega = 0$ in (4), that is, $(\boldsymbol{\Omega} - \boldsymbol{\Lambda} \times \boldsymbol{S}) \times \boldsymbol{S} = 0$, or by solving the eigenvalue equation $\boldsymbol{\Omega} - \boldsymbol{\Lambda} \times \boldsymbol{S} = \lambda\boldsymbol{S}$. It has been shown that the eigenvalue λ of this equation becomes complex in general, where the real part is still equal to the DGD and the imaginary part is given by the frequency derivative of the attenuation difference between the two PSPs (referred to as the differential attenuation slope or DAS) [8]. In this case, the two eigenvectors, i.e., the two modified PSPs, cease to be orthogonal with each other. This indicates that, in a polarization-multiplexed transmission, even when one polarization channel is set as one of the PSPs, the other channel cannot be aligned with the other PSP. Therefore, when the output SOP for one channel is constant in frequency, the output SOP for the other channel inevitably becomes frequency-dependent as shown schematically in Fig. 1(d). This prevents the two channels that are orthogonally polarized before transmission from being completely separated with a polarization beam splitter (PBS) at the receiver, and they are inevitably accompanied by the crosstalk from the other channel. This sets a severe limitation on the transmission performance in a polarization-multiplexed transmission.

B. Influence of PSP Non-Orthogonality in Polarization Demultiplexing

To quantify the magnitude of the crosstalk, here we analytically derive the spectral amplitude that is coupled from the other channel at the polarization demultiplexing. We denote the complex spectral amplitudes of the two channels as $\tilde{A}(\omega)$ and $\tilde{B}(\omega)$, and their Jones vectors as $|A(\omega)\rangle$ and $|B(\omega)\rangle$, respectively. Let $|p\rangle$ be the Jones vector representing the polarization at one port of the PBS. When we receive $\tilde{A}(\omega)$ at this port, we match the SOP at the center frequency ω_0 to the PBS, namely we set $|p\rangle = |A(\omega_0)\rangle$. In this case, the signal from the other channel that couples into the same PBS port is given by the inner product of $|p\rangle$ and $|B(\omega)\rangle$, i.e., $\langle p\,|\,B(\omega)\rangle$. Therefore, the crosstalk component is obtained as

$$\tilde{B}'(\omega) = \langle p\,|\,B(\omega)\rangle \tilde{B}(\omega) \tag{5}$$

and the intensity is given by

$$I_{B\to A}(\omega) = |\tilde{B}'(\omega)|^2 = |\tilde{B}(\omega)|^2 \langle p\,|\,B(\omega)\rangle\langle B(\omega)\,|\,p\rangle. \tag{6}$$

Equation (6) can be rewritten in the following form in terms of Stokes vectors using a conversion formula [17]:

$$I_{B\to A}(\omega) = \frac{1}{2}|\tilde{B}(\omega)|^2(1 + \boldsymbol{p}\cdot\boldsymbol{S}_B(\omega)) \tag{7}$$

where $\boldsymbol{p}$ and $\boldsymbol{S}_B(\omega)$ are the Stokes vectors corresponding to $|p\rangle$ and $|B(\omega)\rangle$, respectively. By noting that the orthogonality between $\tilde{A}(\omega)$ and $\tilde{B}(\omega)$ is only maintained at $\omega = \omega_0$, we can write $\boldsymbol{p} = \boldsymbol{S}_A(\omega_0) = -\boldsymbol{S}_B(\omega_0)$. For a general value of ω, we write $\boldsymbol{S}_B(\omega)$ as a Taylor series expansion around ω_0 up to the second order. As a result, (7) is written as

$$\begin{aligned} I_{B\to A}(\omega) &= \frac{1}{2}|\tilde{B}(\omega)|^2(1 - \boldsymbol{S}_B(\omega_0)\cdot\boldsymbol{S}_B(\omega)) \\ &\cong \frac{1}{2}|\tilde{B}(\omega)|^2 \\ &\quad\times\left\{1 - \boldsymbol{S}_B(\omega_0)\cdot\left(\boldsymbol{S}_B(\omega_0) + \left.\frac{d\boldsymbol{S}_B}{d\omega}\right|_{\omega_0}\Delta\omega \right.\right. \\ &\qquad \left.\left. + \frac{1}{2}\left.\frac{d^2\boldsymbol{S}_B}{d\omega^2}\right|_{\omega_0}\Delta\omega^2\right)\right\} \\ &= -\frac{1}{2}|\tilde{B}(\omega)|^2 \\ &\quad\times\left\{\left(\boldsymbol{S}_B(\omega_0)\cdot\left.\frac{d\boldsymbol{S}_B}{d\omega}\right|_{\omega_0}\right)\Delta\omega \right. \\ &\qquad \left. + \frac{1}{2}\left(\boldsymbol{S}_B(\omega_0)\cdot\left.\frac{d^2\boldsymbol{S}_B}{d\omega^2}\right|_{\omega_0}\right)\Delta\omega^2\right\} \end{aligned} \tag{8}$$

where $\Delta\omega = \omega - \omega_0$ and we use $|\boldsymbol{S}_B(\omega_0)|^2 = 1$. By using (4), it can be shown that the coefficient of $\Delta\omega$ becomes zero:

$$\begin{aligned} \boldsymbol{S}_B\cdot\frac{d\boldsymbol{S}_B}{d\omega} &= \boldsymbol{S}_B\cdot\{\boldsymbol{\Omega}\times\boldsymbol{S}_B - (\boldsymbol{\Lambda}\times\boldsymbol{S}_B)\times\boldsymbol{S}_B\} \\ &= \boldsymbol{S}_B\cdot\{\boldsymbol{\Omega}\times\boldsymbol{S}_B - (\boldsymbol{S}_B\cdot\boldsymbol{\Lambda})\boldsymbol{S}_B + |\boldsymbol{S}_B|^2\boldsymbol{\Lambda}\} \\ &= \boldsymbol{S}_B\cdot(\boldsymbol{\Omega}\times\boldsymbol{S}_B) - |\boldsymbol{S}_B|^2(\boldsymbol{S}_B\cdot\boldsymbol{\Lambda}) \\ &\quad + |\boldsymbol{S}_B|^2(\boldsymbol{S}_B\cdot\boldsymbol{\Lambda}) \\ &= 0. \end{aligned} \tag{9}$$

As regards the coefficient of $\Delta\omega^2$, we obtain

$$\boldsymbol{S}_B\cdot\frac{d^2\boldsymbol{S}_B}{d\omega^2} = -|\boldsymbol{\Omega}\times\boldsymbol{S}_B|^2 - \frac{d\boldsymbol{S}_B}{d\omega}\cdot\boldsymbol{\Lambda}. \tag{10}$$

As a result, we finally obtain the intensity of the crosstalk component as follows:

$$\begin{aligned} I_{B\to A}(\omega) &= \frac{\Delta\omega^2}{4}|\tilde{B}(\omega)|^2 \\ &\quad\times\left\{|\boldsymbol{\Omega}(\omega_0)\times\boldsymbol{S}_B(\omega_0)|^2 + \left.\frac{d\boldsymbol{S}_B}{d\omega}\right|_{\omega_0}\cdot\boldsymbol{\Lambda}(\omega_0)\right\}. \end{aligned} \tag{11}$$

The first term on the right-hand side is derived in [18] as crosstalk induced by PMD, which can be reduced to zero by launching along a PSP, i.e., $\boldsymbol{S}_B(\omega_0)//\boldsymbol{\Omega}(\omega_0)$. In the presence of PDL, the second term newly appears as an additional contribution to the crosstalk. In this case, even if we set $\boldsymbol{S}_B(\omega_0)//\boldsymbol{\Omega}(\omega_0)$, the second term does not vanish. On the other hand, if we set $d\boldsymbol{S}_B/d\omega\,|_{\omega_0} = 0$ instead, which corresponds to matching $\boldsymbol{S}_B$ to PSP in the presence of PDL, the residual crosstalk provided by the first term still exists, and is non-zero despite the PSP launch since $\boldsymbol{\Omega}$ no longer corresponds to PSP any more owing to PDL. Furthermore, the crosstalk from $\tilde{A}(\omega)$ to $\tilde{B}(\omega)$, $I_{A\to B}(\omega)$, is larger than $I_{B\to A}(\omega)$, as the SOP of $\tilde{A}(\omega)$ is not aligned with PSP, i.e., $d\boldsymbol{S}_A/d\omega|_{\omega_0} \neq 0$. This asymmetry is attributed to the existence of PDL. Equation (11) also implies that, for ultrashort optical pulse transmissions, the crosstalk due to PMD and PDL becomes particularly detrimental because of the larger signal bandwidth, $\Delta\omega$.

III. Evaluation of PSP Non-Orthogonality and Crosstalk due to Interplay Between PMD and PDL

A. Polarization Characteristics of Transmission Line

We first measured the PMD and PDL characteristics of a long-haul transmission line that we used in the present work. Each span of the fiber link was composed of a 50 km single-mode fiber (SMF) and a 25 km inverse dispersion fiber (IDF), in which both the dispersion and dispersion slope were compensated. EDFAs compensated for the loss of each span at intervals of 75 km. The experiment was carried out in a straight-line configuration.

The DGD versus wavelength characteristics of a 300 km transmission line that we measured using the Jones matrix eigenanalysis [19] is shown in Fig. 2(a). The mean DGD value was $\Delta\tau = 0.87$ ps. From the differentiation of DGD with respect to wavelength, we can obtain the second-order PMD characteristics. The magnitude of the depolarization $|(\partial\boldsymbol{q}/\partial\omega)\Delta\tau(\omega_0)|$ is plotted in Fig. 2(b) as a function of wavelength. The depolarization value at 1540 nm was 0.27 ps^2. This implies that the direction of PSP, $\boldsymbol{q}$, changes on a Poincaré sphere at a rate $|\partial\boldsymbol{q}/\partial f| = 0.62\pi$ [rad/THz] with respect to frequency, or 0.08π [rad/nm] with respect to wavelength. From

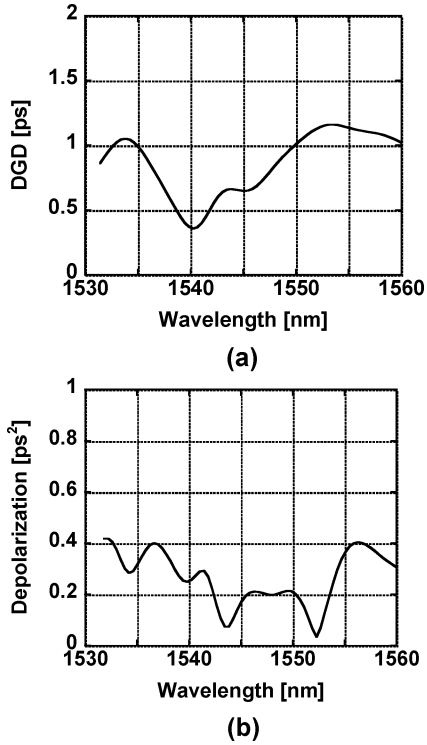

Fig. 2. PMD characteristics of a 300 km transmission link as a function of wavelength. (a) DGD, (b) depolarization.

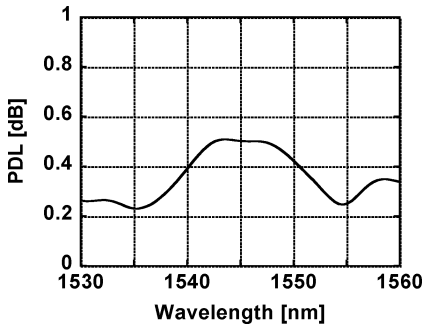

Fig. 3. PDL characteristics of a 300 km transmission link as a function of wavelength.

this result, we estimated that the PSP vector is rotated by 180 deg. within a 13 nm bandwidth.

We also measured the PDL of the entire transmission line. Fig. 3 shows the measured PDL as a function of wavelength. The mean PDL was 0.36 dB, which was generated mainly at the EDFAs.

B. Crosstalk Between Two Polarization Channels

Next we evaluated the crosstalk between polarization channels induced by PMD and PDL during polarization-multiplexed ultrashort pulse propagation. The experimental setup for the evaluation is shown in Fig. 4. We used two types of optical pulses, one was a 1.6 ps pulse directly output from a 40 GHz mode-locked fiber laser (MLFL) and the other was a 0.6 ps pulse, which was compressed externally from the 1.6 ps pulse

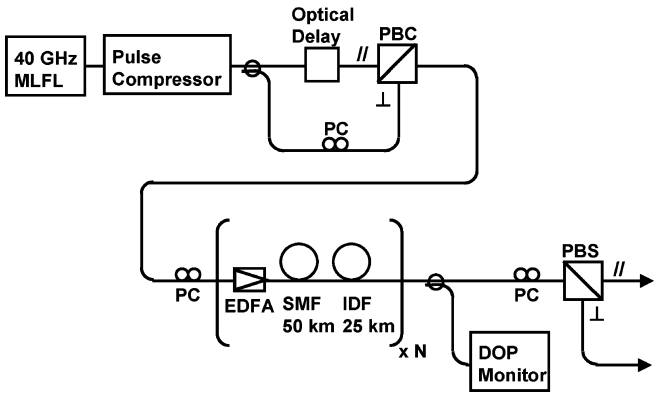

Fig. 4. Experimental setup for evaluating PSP non-orthogonality and crosstalk between two channels.

[20]. The pulsewidth of 0.6 ps is a typical value for 1.28 Tbit/s polarization-multiplexed OTDM transmission (640 Gbaud). The pulse was launched into a fiber link with either a parallel (//) or orthogonal ($\perp$) polarization channel.

We measured the optical power coupled into the other PBS port (//$\rightarrow$ $\perp$ or $\perp$ $\rightarrow$//) at the receiver, and evaluated the crosstalk in a polarization-multiplexed transmission. First, a 0.6 ps pulse was propagated over 300 km with a single, initially parallel, polarization. Before launching the pulse into the transmission line, the input SOP was optimized to match the PSP of the fiber link with a polarization controller (PC) by maximizing the degree of polarization (DOP) after transmission, so that the first-order PMD was mitigated. The SOP prior to PBS was adjusted so that the output power from the // port of the PBS was maximized. Fig. 5 shows the optical spectra measured at each port of the PBS. As we expected, most of the spectrum was output from the // port as shown in Fig. 5(a). At the $\perp$ port, we found that a very small component was leaked from the parallel polarization as shown in Fig. 5(b). This was caused by the residual crosstalk as found in (11).

Next, under the same condition, we simply switched the SOP of the pulse from // to $\perp$ at the transmitter and measured the output from $\perp$ and // ports of the PBS at the receiver. The optical spectra measured at the $\perp$ and // ports are shown in Fig. 6(a) and (b), respectively. If the orthogonality between the two PSPs is preserved, a spectrum identical to Fig. 5 should be obtained because of the symmetry between the two polarizations. However, a larger amount of spectral component was leaked from $\perp$ to //, compared with the leakage from // to $\perp$ shown in Fig. 5(b). At the same time, the spectrum from the $\perp$ port was distorted as shown in Fig. 6(a), where the larger distortion can been seen at the longer wavelength around the spectral peak, corresponding to the larger leakage at the longer wavelength shown in Fig. 6(b). This asymmetry between Figs. 5 and 6 is a consequence of PMD and PDL, and leads to crosstalk at the polarization demultiplexing when the two polarization channels are transmitted simultaneously. In the present case, the crosstalk was estimated to be as large as -12 dB in a 300 km transmission of polarization-multiplexed 0.6 ps pulses, and this includes the combined PMD and PDL effect as well as the crosstalk induced by the

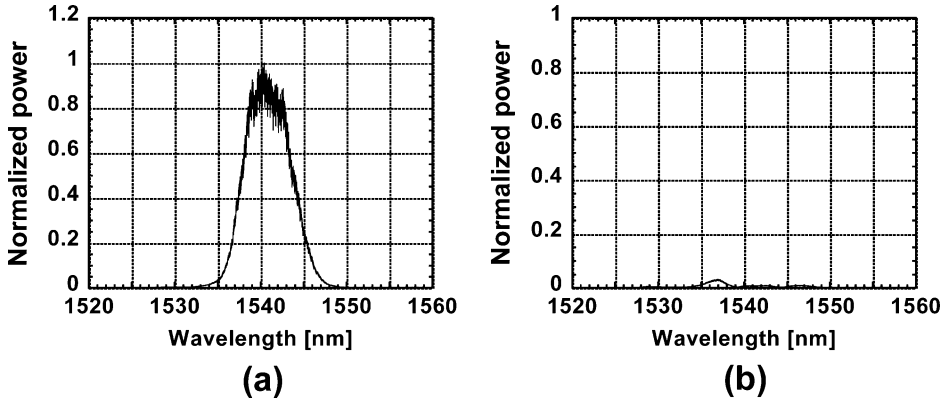

Fig. 5. Optical spectrum of a 0.6 ps pulse after a 300 km transmission when launched along the parallel polarization, measured at // port (a) and ⊥ port (b) of the PBS. SOP is optimized to receive the pulse at maximum power at // port of the PBS. The vertical axes in (a) and (b) indicate the power normalized to the spectral peak in (a).

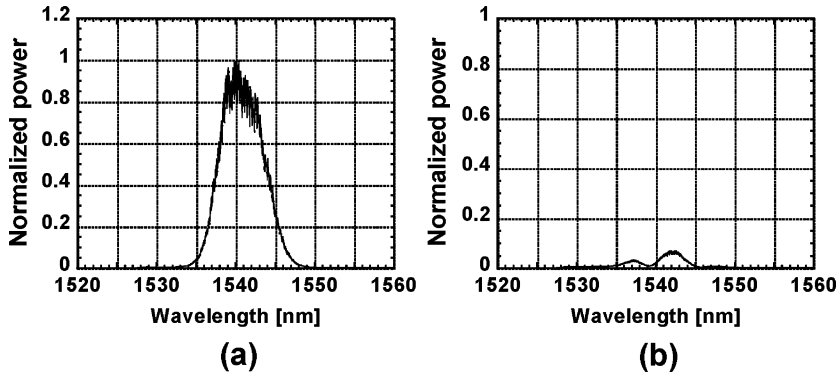

Fig. 6. Optical spectrum of a 0.6 ps pulse after a 300 km transmission when launched along the orthogonal polarization, measured at ⊥ port (a) and // port (b) of the PBS. The vertical axes in (a) and (b) indicate the power normalized to the spectral peak in (a). The SOP optimization is unchanged from the measurement shown in Fig. 5.

second-order PMD itself. Such a large crosstalk is detrimental for terabit/s short pulse transmission over a long distance.

C. PSP Non-Orthogonality

The above experiment also clarified that the input SOP that maximizes the output DOP is slightly different for the two polarization channels. This indicates a decrease in the orthogonality between the two PSPs. So as a next step, we measured the output PSPs for the two polarization channels and evaluated the degree to which the two PSPs deviated from orthogonal, depending on the signal pulsewidth and the transmission length. Specifically, we looked for Stokes parameters of the two PSPs with a polarimeter under individually optimized SOP conditions for // and ⊥ channels, i.e., by maximizing the magnitude of DOP as well as the received optical power through the main port of the PBS. When the two SOPs are orthogonal, the angle between the two Stokes vectors becomes 180 deg., and hence the deviation of the angle from 180 deg. is a measure of the non-orthogonality of the two SOPs. Fig. 7 shows the angle of the two Stokes vectors corresponding to two PSPs, $\boldsymbol{S}_{//}$ and $\boldsymbol{S}_{\perp}$, obtained from

$$\theta = \cos^{-1}\left(\frac{\boldsymbol{S}_{//}\cdot\boldsymbol{S}_{\perp}}{|\boldsymbol{S}_{//}||\boldsymbol{S}_{\perp}|}\right) \tag{12}$$

This result shows that the vector angle starts to decrease after ∼300 km, and the deviation from 180 deg. becomes larger with

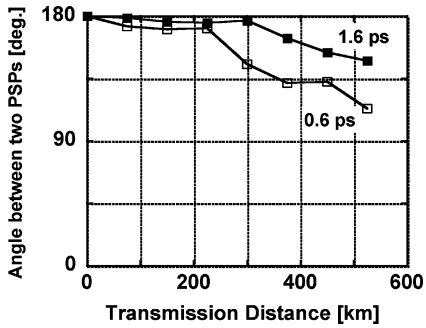

Fig. 7. Decrease in the orthogonality between two PSPs along the transmission distance.

a 0.6 ps pulse, where it is reduced to 113 deg after a 525 km transmission. This phenomenon imposes a severe limitation on the long-haul transmission of polarization-multiplexed ultrashort pulses.

IV. Influence of PMD/PDL-Induced Crosstalk in Polarization-Multiplexed Terabit/s/ch Transmission

To study the system impact of these effects on ultrahigh-speed transmission, we undertook a transmission experiment of a polarization-multiplexed 1.28 Tbit/s/ch (640 Gbaud) DPSK signal over 300 km. The experimental setup is shown in Fig. 8.

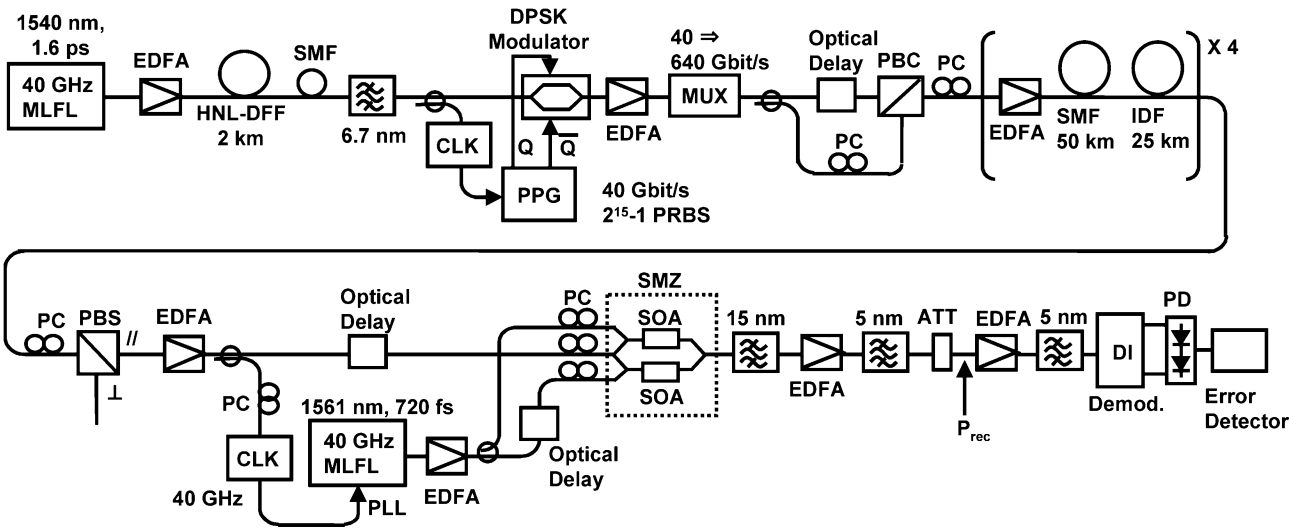

Fig. 8. Experimental setup for 1.28 Tbit/s/ch polarization-multiplexed DPSK transmission over 300 km. Abbreviations are defined in the text.

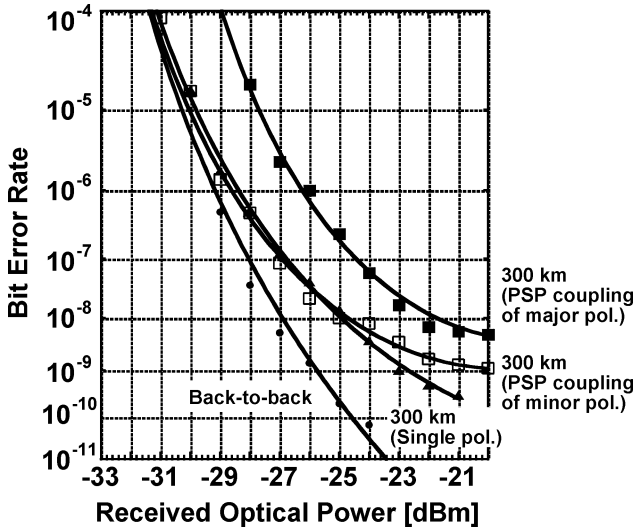

Fig. 9. BER characteristics of a 1.28 Tbit/s-300 km polarization-multiplexed transmission. The closed squares are the results obtained by coupling the main polarization channel to the PSP, and the open squares are obtained by coupling the other polarization channel to the PSP. The triangles show the result for a 640 Gbit/s-300 km single-polarization transmission.

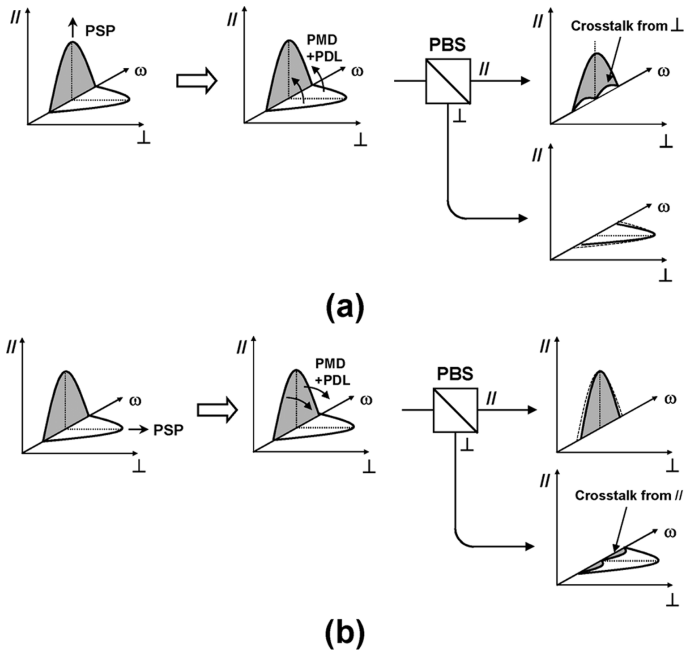

Fig. 10. Crosstalk mechanism induced by the combined effect of PMD and PDL. (a) PSP coupling of major polarization (//), (b) PSP coupling of minor polarization ($\perp$).

In the transmitter, the compressed 40 GHz, 0.6 ps optical pulses, whose wavelength was 1540 nm, were DPSK modulated with a 40 Gbit/s, $2^{15}-1$ PRBS. The DPSK signal was then optically time-division multiplexed to 640 Gbit/s with a single polarization using an optical delay-line multiplexer followed by polarization multiplexing with a polarization beam combiner (PBC). The 1.28 Tbit/s data were then launched into a 300 km transmission fiber. The total dispersion and dispersion slope of the transmission line were precisely compensated with a short piece of SMF at the end of the transmission link. We chose an optimal average input power into each span of $+12$ dBm per polarization to minimize optical signal-to-noise ratio (OSNR) degradation and nonlinear impairments.

On the receiver side, the 1.28 Tbit/s signal was polarization demultiplexed with a PBS, followed by OTDM demultiplexing to 40 Gbit/s with an all-optical semiconductor symmetric Mach–Zehnder (SMZ) switch [21]. As a control pulse source, we used a 40 GHz MLFL emitting a 720 fs pulse. The control pulse wavelength was set at 1561 nm. The MLFL was PLL-operated with a 40 GHz clock extracted from the 640 Gbaud data using an electro-optical PLL clock recovery unit [22]. At the SMZ output, the demultiplexed signal was separated from the control pulse with a 15 nm optical filter. Finally, the demultiplexed 40 Gbit/s DPSK signal was converted to an OOK signal with a one-bit delay interferometer (DI), and the bit error rate (BER) was measured after detection with a balanced photo-detector (PD).

We compared the following two schemes for optimizing the SOP of the launched signal. First, we coupled the main

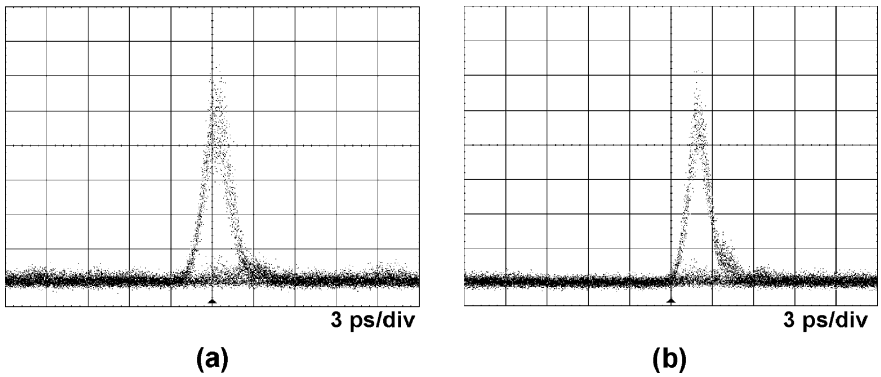

Fig. 11. Waveforms of demultiplexed 40 Gbit/s signal converted to OOK after a 300 km transmission. (a) With conventional polarization demultiplexing, (b) with the present polarization demultiplexing technique.

polarization channel to the PSP and maximized the output power from the main PBS port. The matching of the input SOP to the PSP was carried out by launching the main polarization channel alone and maximizing the DOP after transmission. The BER characteristics after a 300 km transmission are shown by the closed squares in Fig. 9. The result for a single-polarization 640 Gbit/s transmission is also plotted with triangles for comparison. Without PDL, this SOP optimization scheme should yield the optimum polarization demultiplexing for both channels. However, in the presence of PDL, the other channel penetrates the main PBS port because the other channel is not matched to the PSP due to the PSP non-orthogonality, and its SOP is frequency-dependent after transmission. The crosstalk mechanism is shown schematically in Fig. 10(a), where // is assumed to be the main polarization channel in this case. Part of the spectrum in the $\perp$ channel is coupled to the // channel, especially at frequencies away from the center as indicated in (11). As a result, the BER performance is considerably degraded from that of the single-polarization transmission. The received signal waveform is shown in Fig. 11(a), where we can see that the signal indeed suffers from a large impairment especially around the peak and on the trailing edge of the pulse due to the crosstalk.

On the other hand, if we couple the other polarization channel to the PSP and minimize the power at the main PBS port that is coupled from the other polarization, the BER performance is greatly improved as shown by the open squares in Fig. 9. The BER is close to the result obtained with a single polarization. This improvement can be explained as shown schematically in Fig. 10(b). Except for the slight modification in the spectral shape caused by the coupling with the other channel because of the non-PSP launching, the signal does not suffer from impairments. The improvement can also be seen in the received waveform shown in Fig. 11(b). In this case, however, the other polarization channel suffers a large penalty, since part of the power in the desired polarization channel is inevitably leaked to the other PBS port and causes large crosstalk. The performance difference indicated by the difference between the open and closed squares in Fig. 9 corresponds to this asymmetry. Such asymmetry, which cannot be explained by first- or higher-order PMD alone, clearly shows the influence of the combined PMD and PDL effect.

To achieve the same transmission performance for both polarization channels simultaneously, the two polarization channels should be launched to an SOP that is generally different from the PSP so that the DOP after transmission exhibits the same magnitude for both channels, if not a maximum value, but at the expense of depolarization and waveform distortion due to PMD. For practical implementation of polarization-multiplexed signal detection in the presence of PDL, one can adopt a disjoint detection scheme proposed in [23] and [24], in which the polarization-multiplexed signals are first split into two paths by a 3 dB coupler and then optimally detected individually by adjusting a polarizer so as to minimize the light from the other channel, as in the case of Fig. 10(b).

V. Conclusion

We have presented detailed analytical descriptions and experimental demonstrations concerning the influence of PMD and PDL in an ultrahigh-speed polarization-multiplexed transmission. The combined effect of PMD and PDL causes PSPs to be non-orthogonal, and therefore, even when the output SOP for one channel is constant in frequency, that for the other channel is inevitably frequency dependent. This results in crosstalk between two polarizations in polarization-multiplexed ultrashort pulse transmissions. The system impact of these effects was investigated in polarization-multiplexed 1.28 Tbit/s/ch-300 km DPSK transmission, and we found that a large asymmetry could occur in the transmission performance of the two polarization channels. To avoid such impairments, it is important to reduce the bandwidth of the transmitting signal and to minimize the PDL in a long-haul ultrashort pulse transmission.

References

[1] H. G. Weber and M. Nakazawa, Eds.,, *Ultrahigh-Speed Optical Transmission Technology*. Berlin, Germany: Springer, 2007.

[2] M. Nakazawa, T. Yamamoto, and K. R. Tamura, "1.28 Tbit/s-70 km OTDM transmission using third- and fourth-order simultaneous dispersion compensation with a phase modulator," *Electron. Lett.*, vol. 36, no. 24, pp. 2027–2029, Nov. 2000.

[3] H. G. Weber, S. Ferber, M. Kroh, C. Schmidt-Langhorst, R. Ludwig, V. Marembert, C. Boerner, F. Futami, S. Watanabe, and C. Schubert, "Single channel 1.28 Tbit/s and 2.56 Tbit/s DQPSK transmission," *Electron. Lett.*, vol. 42, no. 3, pp. 178–179, Feb. 2006.

[4] C. D. Poole, "Polarization effects in lightwave systems," in *Optical Fiber Telecommunications III A*, I. P. Kaminow and T. L. Koch, Eds. New York: Academic, 1997, ch. 6.

[5] H. Kogelnik, L. E. Nelson, and R. M. Jopson, "Polarization mode dispersion," in *Optical Fiber Telecommunications IV B*, I. P. Kaminow and T. Li, Eds. New York: Academic, 2002, ch. 15.
[6] G. J. Foschini, R. M. Jopson, L. E. Nelson, and H. Kogelnik, "The statistics of PMD-induced chromatic fiber dispersion," *J. Lightw. Technol.*, vol. 17, no. 9, pp. 1560–1565, Sep. 1999.
[7] G. J. Foschini, L. E. Nelson, R. M. Jopson, and H. Kogelnik, "Statistics of second-order PMD depolarization," *J. Lightw. Technol.*, vol. 19, no. 12, pp. 1882–1886, Dec. 2001.
[8] N. Gisin and B. Hutter, "Combined effects of polarization mode dispersion and polarization dependent loss in optical fibers," *Opt. Commun.*, vol. 142, pp. 119–125, Oct. 1997.
[9] M. Shtaif and O. Rosenberg, "Polarization-dependent loss as a waveform-distorting mechanism and its effect on fiber-optic systems," *J. Lightw. Technol.*, vol. 23, no. 2, pp. 923–930, Feb. 2005.
[10] A. Mecozzi and M. Shtaif, "Signal-to-noise-ration degradation caused by polarization-dependent loss and the effect of dynamic gain equalization," *J. Lightw. Technol.*, vol. 22, no. 8, pp. 1856–1871, Aug. 2004.
[11] J. Renaudier, G. Charlet, M. Salsi, O. B. Pardo, H. Mardoyan, P. Tran, and S. Bigo, "Linear fiber impairments mitigation of 40-Gbit/s polarization-multiplexed QPSK by digital processing in a coherent receiver," *J. Lightw. Technol.*, vol. 26, no. 1, pp. 36–42, Jan. 2008.
[12] M. Shtaif, "Performacne degradation in coherent polarization multiplexed systems as a result of polarization dependent loss," *Opt. Exp.*, vol. 16, no. 18, pp. 13918–13932, Sep. 2008.
[13] C. Zhang, Y. Mori, M. Usui, K. Igarashi, K. Katoh, and K. Kikuchi, "Straight-line 1 073-km transmission of 640-Gbit/s dual-polarization QPSK signals on a single carrier," in *Proc. Eur. Conf. Opt. Commun.*, Vienna, Austria, 2009, Postdeadline paper PD2.8.
[14] C. Schmidt-Langhorst, R. Ludwig, D.-D. Gross, L. Molle, M. Seimetz, R. Freund, and C. Schubert, "Generation and coherent time-division demultiplexing of up to 5.1 Tb/s single-channel 8-PSK and 16-QAM signals," in *Proc. Opt. Fiber Commun. Conf.*, San Diego, CA, Mar. 2009, Postdeadline paper PDPC6.
[15] K. Kasai, T. Omiya, P. Guan, M. Yoshida, T. Hirooka, and M. Nakazawa, "Single-channel 400-Gb/s OTDM-32 RZ/QAM coherent transmission over 225 km using an optical phase-locked loop technique," *IEEE Photon. Technol. Lett.*, vol. 22, no. 8, pp. 562–564, Apr. 2010.
[16] Y. Li and A. Yariv, "Solutions to the dynamical equation of polarization-mode dispersion and polarization-dependent losses," *J. Opt. Soc. Amer. B*, vol. 17, no. 11, pp. 1821–1827, Nov. 2000.
[17] J. P. Gordon and H. Kogelnik, "PMD fundamentals," in *Proc. Nat. Acad. Sci.*, 2000, vol. 97, pp. 4541–4550.
[18] L. E. Nelson, T. N. Nielsen, and H. Kogelnik, "Observation of PMD-induced coherent crosstalk in polarization-multiplexed transmission," *IEEE Photon. Technol. Lett.*, vol. 13, no. 7, pp. 738–740, Jul. 2001.
[19] B. L. Heffner, "Accurate, automated measurement of differential group delay dispersion and principal state variation using Jones matrix eigenanalysis," *IEEE Photon. Technol. Lett.*, vol. 5, no. 7, pp. 814–817, Jul. 1993.
[20] T. Hirano, P. Guan, T. Hirooka, and M. Nakazawa, "640 Gbit/s/channel single-polarization DPSK transmission over 525 km with ultrafast time-domain optical Fourier transformation," *IEEE Photon. Technol. Lett.*, vol. 22, no. 4, pp. 1042–1044, Jul. 2010.
[21] K. Tajima, "All-optical switch with switch-off time unrestricted by carrier lifetime," *Jpn. J. Appl. Phys.*, vol. 32, no. 12A, pp. L1746–L1749, Dec. 1993.
[22] C. Boerner, V. Marembert, S. Ferber, C. Schubert, C. Schmidt-Langhorst, R. Ludwig, and H. G. Weber, "320 Gbit/s clock recovery with electro-optical PLL using a bidirectionally operated electroabsorption modulator as phase comparator," in *Proc. Opt. Fiber Commun. Conf.*, Anaheim, CA, Mar. 2005, Paper OTuO3.
[23] A. Chraplyvy, A. H. Gnauck, R. W. Tkach, J. L. Zyskind, J. W. Sulhoff, A. J. Lucero, Y. Sun, R. M. Jopson, F. Forghieri, R. M. Derosier, C. Wolf, and A. R. McCormick, "1-Tb/s transmission experiment," *IEEE Photon. Technol. Lett.*, vol. 8, no. 9, pp. 1264–1266, Sep. 1996.
[24] A. Andrusier and M. Shtaif, "Disjoint detection in polarization multiplexed communication systems affected by polarization dependent loss," *Opt. Exp.*, vol. 17, no. 10, pp. 8173–8184, May 2009.

Toshihiko Hirooka (M'00) received the Ph.D. degree in electronics and information systems engineering from Osaka University, Osaka, Japan, in 2000.

During 2000–2002, he was a Research Associate with the Department of Applied Mathematics, University of Colorado at Boulder. He is currently an Associate Professor with the Research Institute of Electrical Communication, Tohoku University, Sendai, Japan. He has been engaged in research on ultrahigh-speed optical communications and nonlinear fiber optics, including OTDM transmission, optical solitons, and photonic crystal fibers.

Dr. Hirooka is a member of the Optical Society of America, the IEICE, and the Laser Society of Japan.

Toshiyuki Hirano received the B.S. degree in communications engineering from Tohoku University, Sendai, Japan, in 2009, where he is currently working toward the M.S. degree.

His research interests include ultrahigh-speed optical communication.

Yutaro Tomiyama received the B.S. degree in communications engineering from Tohoku University, Sendai, Japan, in 2010, where he is currently working toward the M.S. degree.

His research interests include ultrahigh-speed optical communication.

Pengyu Guan (S'09) received the B.S. degree in photonics engineering from Ritsumeikan University, Kusatsu, Japan, in 2007, and the M.S. degree in communications engineering from Tohoku University, Sendai, Japan, in 2009, where he is currently working toward the Ph.D. degree.

Currently he is a Research Fellow of the Japan Society for the Promotion of Science (JSPS), studying toward his Ph.D. at the Research Institute of Electrical Communication, Tohoku University. His research interests include ultrahigh-speed optical communication.

Masataka Nakazawa (F'95) received the Ph.D. degree from the Tokyo Institute of Technology, Tokyo, Japan, in 1980.

He then joined the Ibaraki Electrical Communication Laboratory of Nippon Telegraph and Telephone (NTT) Corporation, where he engaged in research on EDFAs, soliton transmission, and Terabit/s OTDM transmission. He was a Visiting Scientist with MIT from 1984 to 1985. In 2001, he became a Professor with the Research Institute of Electrical Communication, Tohoku University, Sendai, Japan, and was promoted to a Distinguished Professor in 2008. He is now the Director of the Institute. He has published more than 400 papers and given 230 international conference presentations.

Dr. Nakazawa has received many awards including the IEE Electronics Letters Premium Award, the IEEE Daniel E. Noble Award, the OSA R. W. Wood Prize, the Thomson Scientific Laureate, and the IEEE Quantum Electronics Award.